Investigation of a Damaged High-rise Building near Ground Zero

Gordon Warn
Department of Civil, Structural & Environmental Engineering
State University of New York at Buffalo

Jeffrey Berman
Department of Civil, Structural & Environmental Engineering
State University of New York at Buffalo

Andrew Whittaker
Department of Civil, Structural & Environmental Engineering
State University of New York at Buffalo

Michel Bruneau
Multidisciplinary Center for Earthquake Engineering Research
State University of New York at Buffalo

Introduction

Within two weeks of the September 11, 2001, attacks on the World Trade Center towers in New York City, the Multidisciplinary Center for Earthquake Engineering Research (MCEER) dispatched a research team to the site to collect perishable data related to the collapse of the two 110-story towers and collateral damage to buildings and infrastructure surrounding the World Trade Center complex. Two visits to Ground Zero were undertaken, the first on September 21 (see Bruneau et al. (2002)) and the second on September 23. The visit on September 23 involved a walk-through of one high-rise building that was badly damaged by large pieces of debris that were ejected from World Trade Center tower 2 as it collapsed.

The objectives of the work described in this paper were two-fold: (1) to collect information about the structural and nonstructural damage suffered by the building at 130 Liberty Plaza due to the collapse of tower 2, and (2) to investigate whether simple numerical tools used in the structural analysis of buildings can be used to help explain the observed structural behavior. The first objective was achieved by the September 23 walk-through of the building. Summary information on the building damage is presented in the reconnaissance section. The second objective was addressed using linear and nonlinear analysis tools that are used by earthquake engineers. Berman et al. (2002) and Warn et al. (forthcoming) present detailed information on the September 23 reconnaissance and the subsequent studies.

The building studied is a 39-story office building at 130 Liberty Street in lower Manhattan. It was located to the immediate south of tower 2. Figure 1 shows the building's location with respect to the Trade Center complex.

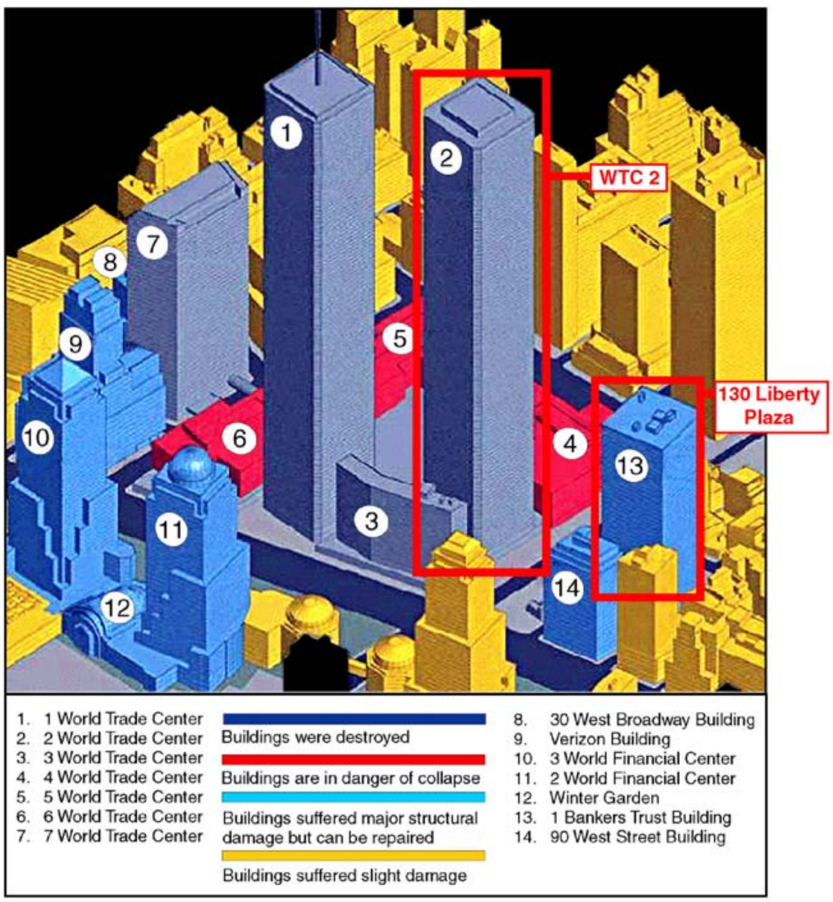

Figure 1. Location of subject building with respect to the World Trade Center complex.

The 130 Liberty Street building was designed in the early 1970s by the structural engineering firm of James Ruderman LLP. Structural drawings were not available to the reconnaissance team from the building owner but information on the framing system was gathered during the reconnaissance. The typical gravity framing system is composed of a non-composite unreinforced concrete slab on metal decking spanning approximately 8 feet 8 inches to steel beams that span 26 feet to steel girders that frame into steel wide-flange columns. The concrete slab is 2.5 inches thick atop a 20-gauge metal deck. The lateral framing system consists of a three-dimensional steel moment-resisting space frame (that is, all beam-to-column connections are rigid connections) and a steel braced core. Figure 2 shows a part plan of a typical floor; the member sizes indicated on the figure were established by members of the reconnaissance team after independent analysis of the frame as described in the building analysis section. The grid marks (A through H and 1 through 8) were selected by the reconnaissance team to aid in the identification and interpretation of damage.

The façade of the building consists of windows and a lightweight cladding system. A sketch of the northern façade badly damaged by falling debris is presented in Figure 3. The elliptical line in the figure identifies the zone of damage to the façade of the building, where TL denotes "tenant level."

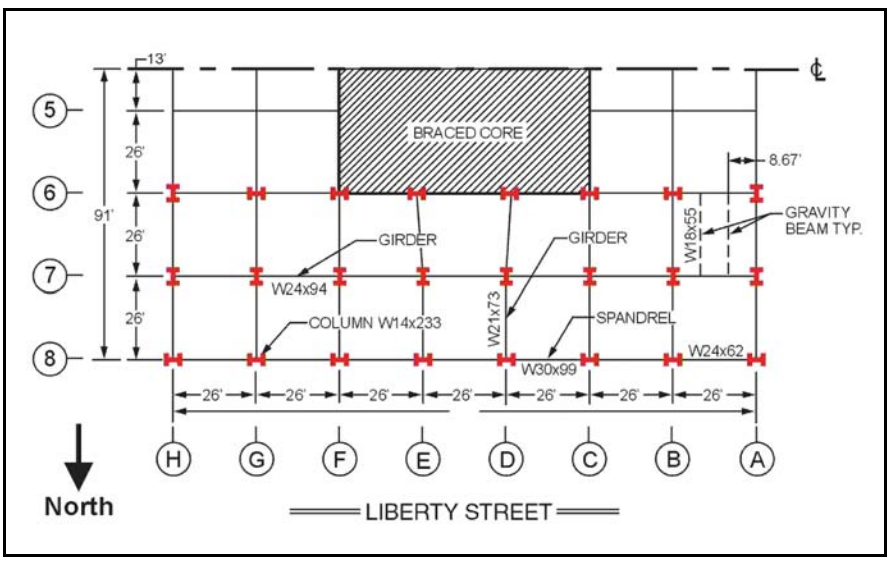

Figure 2. Part plan view of a typical floor with estimated section sizes at tenant level 25.

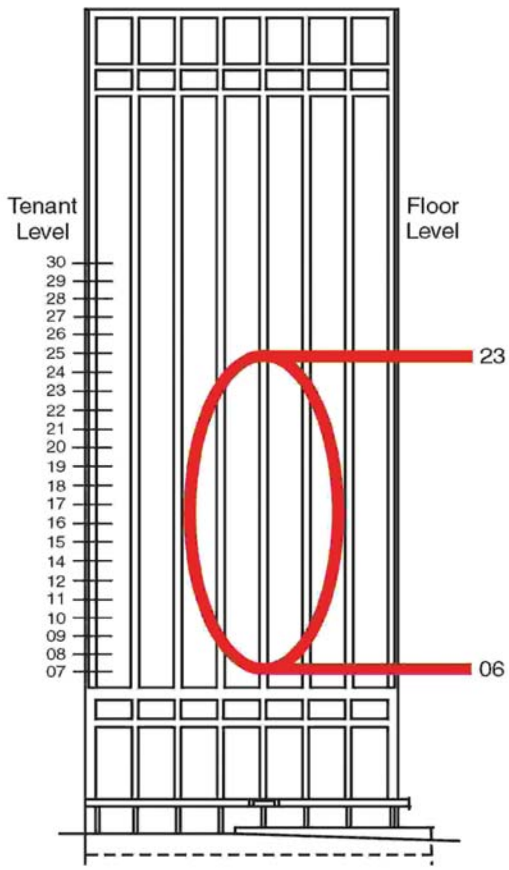

Figure 3. Sketch of northern façade showing the zone of damage.

Reconnaissance

Exterior Reconnaissance of September 21, 2001

The visit of September 21 involved an exterior inspection of the building from ground level as part of a broader survey reported elsewhere (Bruneau et al., 2002). Figure 4 presents four photographs of the building taken on September 21, 2001. Part a. is a view of the northern façade showing the large gash in the exterior wall caused by falling debris that was ejected from tower 2 as it collapsed. One large piece of the façade of tower 2 can be seen in this figure at approximately the 9th floor level. It is highly likely that this three-story-high piece of debris caused much of the damage that is evident above the 9th floor. Clearly seen in this figure is the loss of a column on line D (see Figure 2) between tenant level 7 and tenant level 25.

Part b of Figure 4 shows damage to the northern and western faces of the building. Windows were broken on both of these faces of the building but the damage on the western face was confined to a one-bay width between lines 7 and 8. The cladding to corner column A8 was lost between the ground and tenant level 5 and between tenant level 9 and 12.

Parts c and d of Figure 4 show damage to the lower levels of the building on its north face. Burning debris ignited small fires in the lower levels of the building but these fires appear to have been confined to the perimeter of the building. Most of the windows in the lower levels, especially below the mechanical plant room at the 5th floor, were broken but it is not known how many of these windows were broken deliberately by the rescue teams to eliminate falling glazing hazards to the rescue workers operating to

Figure 4a. Damage to the 130 Liberty Plaza building from the exterior—view of northern façade.

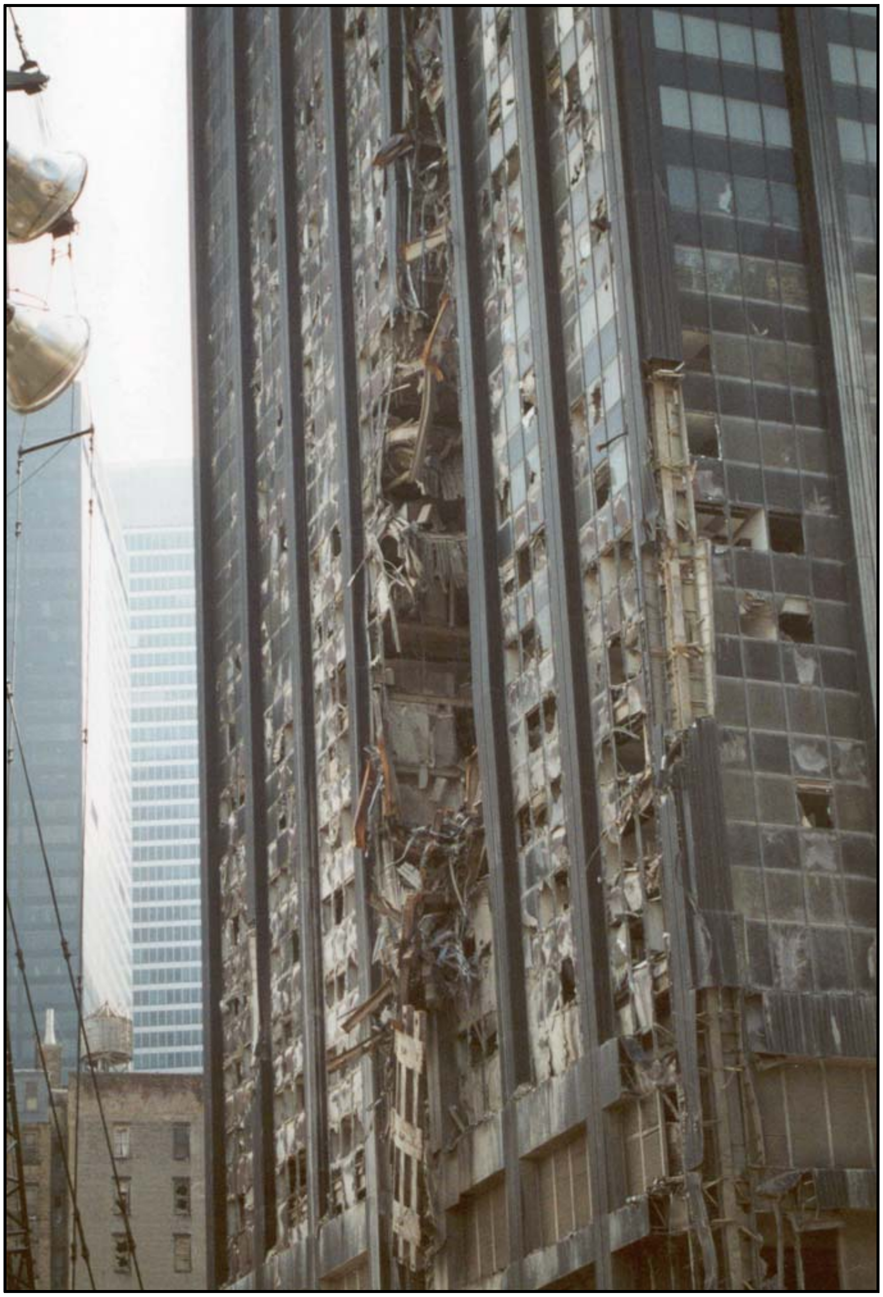

Figure 4b. Damage to the 130 Liberty Plaza building from the exterior—view of northern and western facades.

***Figure 4c. Damage to the 130 Liberty Plaza building from the exterior—view of lower 10 stories of northern façade*.**

Figure 4d. Damage to the 130 Liberty Plaza building from the exterior—damage to northern façade at the entry level.

the immediate south of tower 2. Part d shows the debris pile just north of the building, 10 days after the attacks. Much of the debris was from tower 2.

Figure 5 presents information on the moment-resisting connections used in the building. Part a of the figure shows fire damage to the lower framing, a cover-plated moment connection of the beam to the column, and the connections used to join the steel floor beams to the perimeter girders. No spray-on fireproofing is evident on the side or bottom of the perimeter beam although it may have been knocked off upon impact. Façade construction details can be clearly seen in this figure. Part b of the figure shows a typical beam-column moment connection on the western face of the building. Cover plates are clearly visible in this connection and damaged (or incomplete) fireproofing can be seen on the exterior face (web) of the perimeter beam.

Interior Reconnaissance of September 23, 2001

One member of the MCEER reconnaissance team returned to Ground Zero on September 23, 2002, to accompany an expert structural engineer from LZA/Thornton Tomasetti on a detailed inspection of the interior of the building. That inspection involved climbing directly from the entry level to the roof via the two stairwells located in the core of the building and returning to the entry level after a floor-by-floor inspection of the building, in which all quadrants of the building were inspected at each floor but with attention being focused on that portion of every floor to the north of grid 6.

Figure 5a. Exposed steel moment framing in the first story of the building—first story of northern face.

Figure 5b. Exposed steel moment framing in the first story of the building—first story of the western face.

Both structural and non-structural components in the building suffered significant damage but all of the non-dust- and non-mildew-related damage above the sixth floor appeared to be substantially confined to a two-bay-by-two-bay zone contained by lines 6 and 8 and C and E (see Figure 2 for details). Non-structural damage did extend a short distance to the west of line C and the east of line E.

Figure 6 presents photographs taken at the roof level of the building. Part a of the figure is a photograph looking east across the roof. Silver U-shaped aluminum panels from tower 2 can be seen in the figure together with life vests from American Airlines (AA) Flight 11 that struck the north face of tower 1 (approximately 120 meters from 130 Liberty Plaza). Part b of the figure is a photograph looking west across the roof. Aluminum panels and AA life vests are also visible in this figure. Parts c and d of the figure are close-up photographs of an AA life vest and a seat from the AA Flight 11.

No structural damage was observed at the roof level of the building and there was no evidence that the roof floor slab had been punctured by falling debris from tower 2. This observation was confirmed by the walk-though of the plant-room spaces immediately below the roof. Apart from broken glass in the stairwells from the roof-level skylights, the structure and mechanical plant in the 38th story were undamaged by the collapse of tower 2.

Figure 6a. Debris at the roof level of 130 Liberty Plaza—photograph looking east.

Figure 6b. Debris at the roof level of 130 Liberty Plaza—photograph looking west.

Figure 6c. Debris at the roof level of 130 Liberty Plaza—American Airlines life vest.

Figure 6d. Debris at the roof level of 130 Liberty Plaza—seat from American Airlines plane.

Figure 7a. Office space damage above tenant level 29 — penetration of tower 2 fascia piece.

Figure 7b. Office space damage above tenant level 29— typical damage in office space.

Damage to the building above tenant level 29 was modest (relative to the damage below tenant level 25) and was limited to broken glass (caused by debris ejected from tower 2 as it collapsed). Figure 7 shows sample non-structural damage above tenant level 29. Part a of the figure shows damage caused by a section of fascia that was ejected from tower 2 and penetrated a window on the northern face of the building. Part b shows debris in a corner office at grid A8. The angle section lying atop the overturned chair in this figure penetrated the north-facing window of the building. (The hard hat and flashlight in the photograph belonged to the photographer.)

The first major structural damage was observed at tenant level 29 and was due to the impact of one single-story-tall structural steel column from tower 2. (As described in Bruneau et al. (2002), this column was one of three in a typical spandrel module, so the two steel beams linking the three columns were destroyed before the single column hit the 130 Liberty Plaza building.) Figure 8a is a sketch of a typical three-column module. Figure 8b shows the upper end of the column above Level 29. Figure 8c is a photograph of the underside of the column and the damage it caused to the ceiling system. It is noteworthy that the unreinforced slab on metal deck arrested the fall of this substantial steel member.

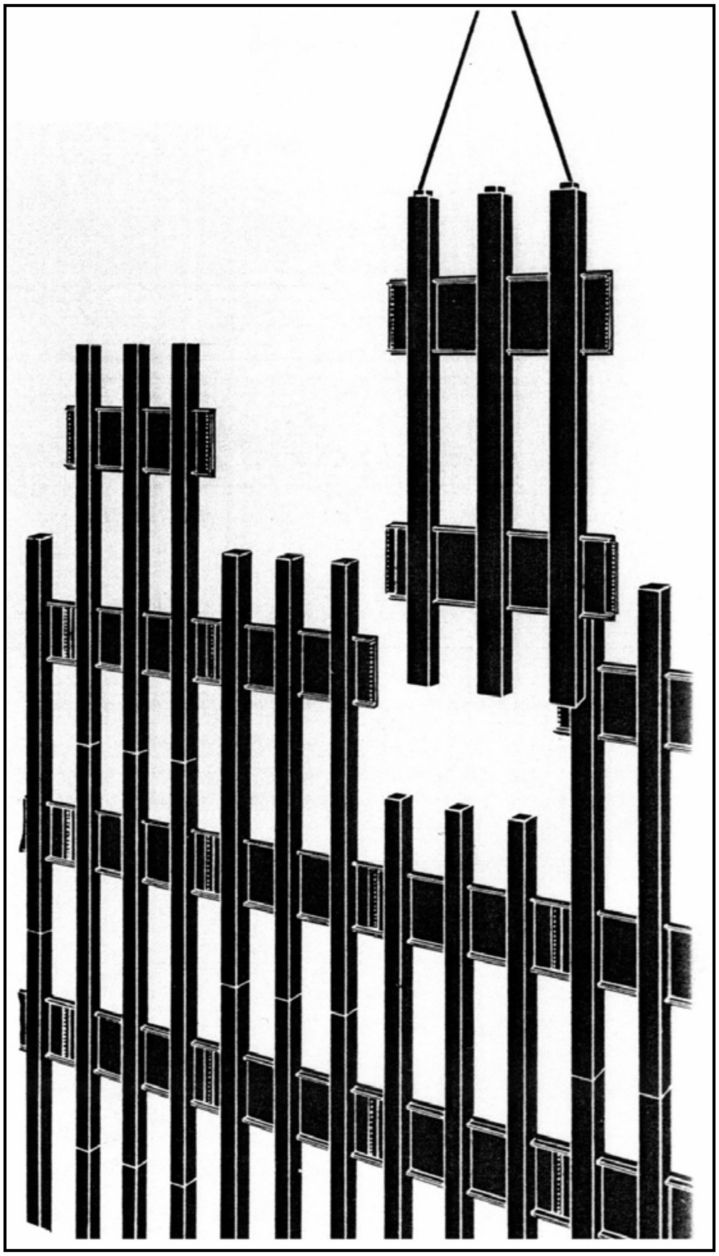

Figure 8a. Damage due to column-missile ejected from tower 2—three-column module used in the construction of tower 2 (from Hart et al., 1978).

Figure 8b. Damage due to column-missile ejected from tower 2—upper end of column-missile above level 29.

***Figure 8c. Damage due to column-missile ejected from tower 2—
Lower end of column-missile below level 29.***

There was little evidence of damage to or distress in the building frame in the stories immediately above the zone of structural damage. There was no sign of excessive deflection in the framing above tenant level 25 as evinced by the total lack of deflection-induced damage in brittle components such as glazing and plasterboard partitions.

The degree of damage to the structural framing increased substantially below tenant level 26. Figure 9a shows a north-south spanning floor beam at the underside of tenant level 23 that has lost its support on line 8 due to the failure (loss) of the spandrel beam between lines D and E. Note the clean separation of the metal deck from the beam (made possible by the lack of studs joining the beam to the slab). Part b of the figure shows the underside of the floor slab at tenant level 22. At this level both north-south spanning floor beams were lost; the locations of these beams are marked by dark stripes on the underside of the metal decking. Of importance to the integrity of the floor system is the fact that the tenant level 22 slab at this location was able to span three times the distance assumed in design, namely, 26 feet, albeit with large deflections in the slab system. Part c of the figure shows a view of the slab of part b looking north-east. Part d of the figure is a view looking northeast of the underside of the slab at tenant level 21: a photograph taken from

Figure 9a. Interior damage at tenant levels 22 and 21—underside of level 23 slab looking northwest.

Figure 9b. Interior damage at tenant levels 22 and 21—underside of level 22 slab looking northwest.

Figure 9c. Interior damage at tenant levels 22 and 21—underside of level 22 slab looking northeast.

Figure 9d. Interior damage at tenant levels 22 and 21—underside of level 21 slab looking northeast.

approximately the same location as Figure 9c but one floor lower in the building. Fracture of the metal deck floor system at the line of the girder spanning north-south on line E can be seen in part d of the figure together with gross distortion of two steel floor beams spanning north-south to the (lost) spandrel.

Figure 10 shows the remnants of a moment-resisting connection as photographed from tenant level 19 in the building. The fractured flange connections and the welded web tab are clearly visible. Part b of the figure is a photograph taken from the same location as the photograph of part a but looking towards the north-south spanning girder on line C. The World Financial Center and Winter Garden can be seen in the background of this photograph. Figure 10c is a view of two stories of framing along line D. Note the distortion in the column flanges at the level of the beam-to-column connection and that the metal decking fractured cleanly along a butt (noncontinuous) joint atop the girder on line D. Large deflections in the floor framing are not seen in this figure. Part d of the figure shows the fractured column on line D at approximately three feet above tenant level 18, immediately below the bottom of the framing shown in part c of the figure. The rubble pile at the base of tower 2 can be seen in the bottom of the Figure 10d.

Figures 11a and 11b are photographs of the fractured column on line D taken from tenant levels 18 and 17, respectively. The façade of tower 2 can be seen in the background of part a of the figure and World Trade Center 4 can be seen in the background of part b of the figure.

Figure 12 presents two photographs taken from outside the building looking toward the damage zone described in the previous pages. The box superimposed on Figure 12a shows the column of Figure 11. The fracture evident in Figure 11a is located at the top of the box. The distorted but intact two-story section of column seen in Figure 11b is located in the center of the box. In Figure 12a, the upper dashed line is at tenant level 25 and the lower dashed line is at tenant level 7. The dashed line in Figure 12b corresponds to the lower dashed line of Figure 12a. The large piece of debris that likely caused most of the damage above tenant level 10 is seen in Figure 12b precariously attached to the façade of the building.

The damage to the structural and non-structural components between tenant levels 16 and 10 was most severe. The near-total destruction of the ceiling, mechanical, and plumbing systems in the areas surrounding the collapsed structural framing prevented the reconnaissance team from gaining access to the perimeter of the damage zone. As seen in Figures 12a and 12b, the zone of extreme damage expanded below tenant level 16 to the two-bay-by-two-bay zone bounded by lines C and E and 6 and 8.

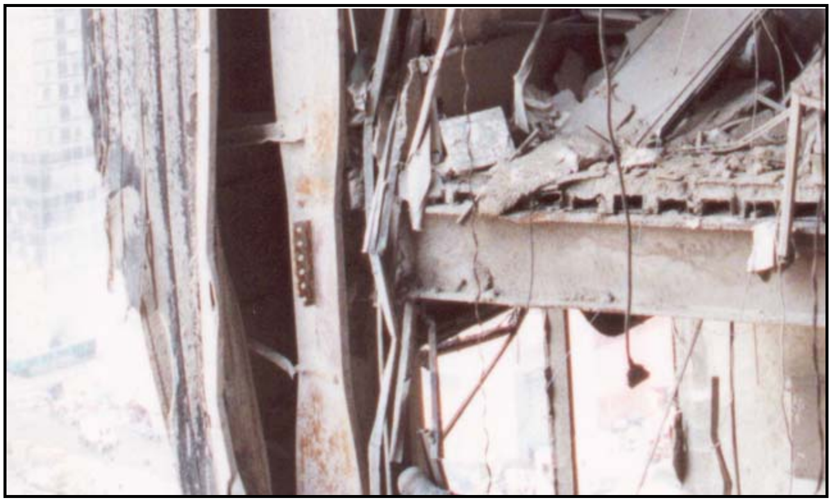

Figure 10a. Interior damage photographs from tenant level 19—failed moment connection at grid D8.

Figure 10b. Interior damage photographs from tenant level 19—floor framing on line 8 between lines C and D.

Figure 10c. Interior damage photographs from tenant level 19—damaged framing at levels 19 and 20.

Figure 10d. Interior damage photographs from tenant level 19—failed column immediately above level 18.

Figure 11a. Fractured column on line D from tenant levels 18 and 17—view at level 18.

Figure 11b. Fractured column on line D from tenant levels 18 and 17—view at level 17.

Figure 12a. Damage to the northern face of the building between tenant levels 23 and 10— view of damage zone between levels 23 and 10.

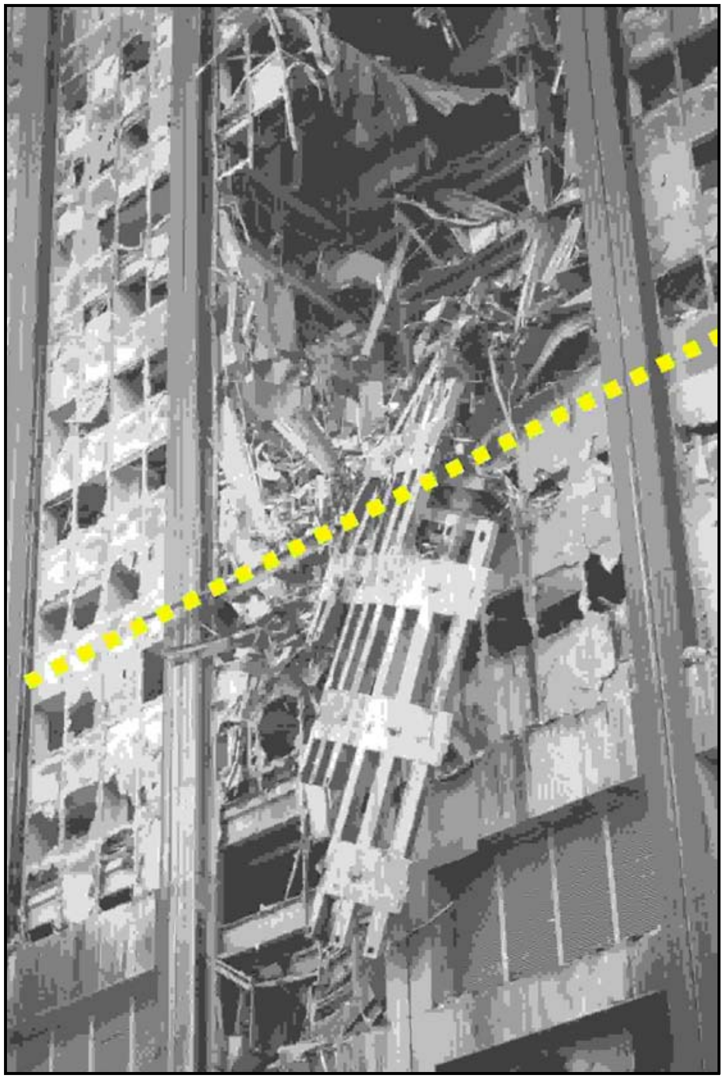

Figure 12b. Damage to the northern face of the building between tenant levels 23 and 10—view of damage zone adjacent to level 10.

Figure 13 shows two photographs of damage at tenant level 9. Figure 13a shows the complete destruction of one zone of the floor immediately adjacent to the northern face of the building. Part b of the figure shows the interior face of the section of tower 2 façade seen in Figures 4a and 12b that caused much of the damage to the building.

Structural damage below the mechanical plant rooms that were located below tenant level 9 was modest and no photographs were taken at the levels between tenant level 9 and the entryway to the building. Figure 14 is a photograph taken inside the building looking north towards a standing section of the tower 2 façade.

Building Analysis

The observation that the subject building did not collapse despite the loss of key structural elements and severe damage motivated the research team to analyze the building to understand the cause of the observed behavior. Standard tools for the linear and nonlinear analysis of buildings subjected to earthquake shaking were employed for these studies. Linear analysis was performed to determine demand-to-capacity ratios for an undamaged state as well as three damage states, one of which corresponds to the observed damage. Linear analysis further provided an estimate of the elastic limit of the framing system for each of the damage states considered. Two-dimensional and three-dimensional linear analyses were performed. Small displacement theory was employed for these analyses. Simple plastic analysis was then performed to determine an upper bound to the capacity of the framing system for each of the damage states considered. Both two- and three-dimensional framing systems were considered for simple plastic analysis.

Detailed information on the structural framing system was not available to the research team, although approximate sizes were noted during the building reconnaissance. To facilitate the linear and nonlinear analysis of the building, sizes of the beams and columns in the moment-resisting frame were estimated by analysis of the building frame for gravity and winds loads as described in the following section. All beam-to-column connections were assumed to be moment resisting. The estimated sizes of the W-shape beams and columns were checked against the approximate sizes noted during the building reconnaissance. Because no information was available on the steel braced core, sizes were not estimated for the steel braces.

Figure 13a. Building damage at tenant level 9—complete destruction of one zone of the building.

Figure 13b. Building damage at tenant level 9—view of inside face of tower 2 façade element.

Figure 14. View of the tower 2 façade looking northwest from the foyer of the building.

Preliminary Analysis and Design

A preliminary design was undertaken per the 1970 Building Code of the City of New York (City of New York, 1970) to determine beam and column section sizes. Resulting sizes of the beams and columns were used in the analytical studies presented herein. Because actual sizes were unavailable, the reader should interpret the analysis results presented below with care with regards to the performance of the 130 Liberty Plaza building.

Both gravity and wind loads were considered for the preliminary design. Gravity loads were taken to be 50 pounds per square foot (psf) (dead load) and 100 psf (live load), based on measured structural properties and the occupancy of the building. Live loads were reduced for the design of columns. Wind pressures on the face of the building were taken to be 30 psf for elevations above 301 feet, 25 psf for elevations between 101 feet and 300 feet, and 20 psf for elevations below 100 feet. A one-third increase in allowable stress was used for the gravity and wind load combinations per the 1970 building code. Limits on maximum lateral drift under wind loads were not considered.

Only the moment-resisting frame along line 8 (see Figure 2) was considered for preliminary analysis and design. The tributary building width for calculating wind loads for the line 8 frame was taken to be 39 feet: one and one-half bay widths. Design actions were first estimated using simple analysis tools, including the portal method. Steel sections were then sized using the *Manual of Steel Construction— Allowable Stress Design* (American Institute of Steel Construction, 1989).

To facilitate three-dimensional finite element analysis of the building, sections sizes along frame lines 6 and 7, including intermediate perpendicular framing, were determined based on information from the September 23, 2001, reconnaissance visit and gravity load considerations. The resulting column and beam sections at tenant level 25 are shown in Figure 2 for one-half of a typical building floor plan.

Linear Elastic Analysis

Two- and three-dimensional finite element models were constructed using SAP2000 (Computers and Structures, Inc., 2000). First, a two-dimensional model (Figure 15a) was prepared that considered structural framing over all 39 stories along line 8 (see Figure 2). This model was constructed to study the response of a single frame with varying degrees of damage (or damage states). Second, a three-dimensional model was prepared that considered structural framing over all 39 stories along lines 6, 7, and 8, including intermediate perpendicular framing (Figure 16). This model was prepared to better understand the response of the building for the observed damage state and to

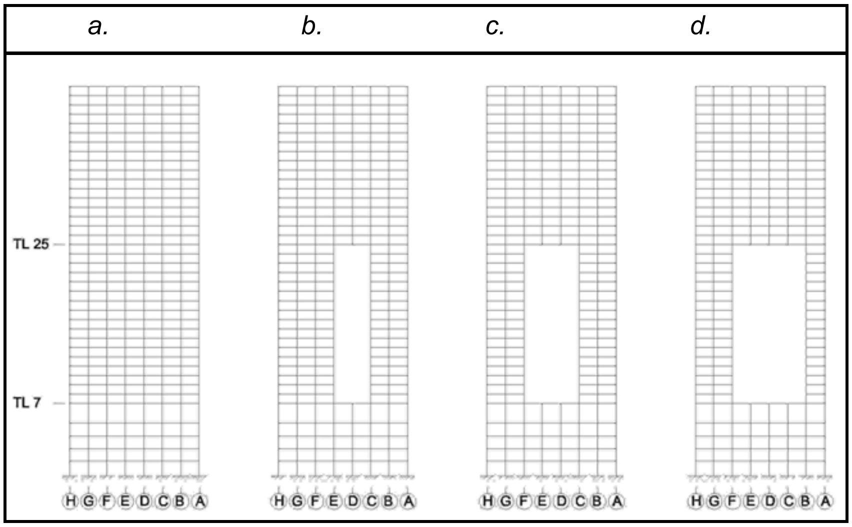

Figure 15. Two-dimensional mathematical models of framing on Line 8: a. ND model; b. DS1 model; c. DS2 model; d. DS3 model.

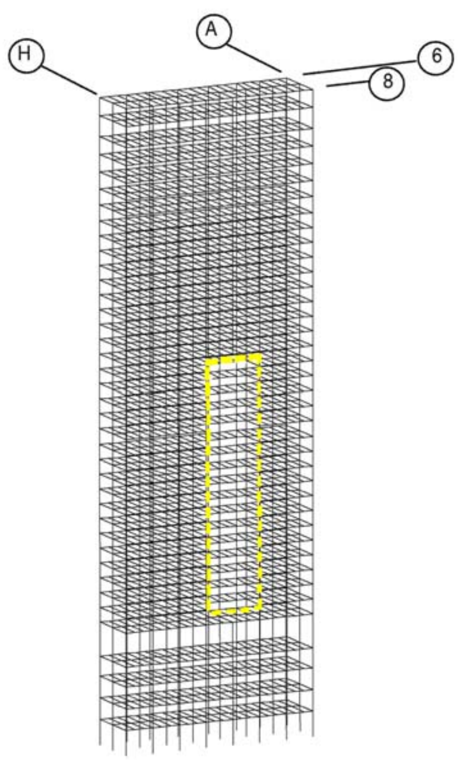

compare the results of two- and three-dimensional analysis. The light dashed line in Figure 16 identifies the zone of observed damage per Figure 15b.

The analyses presented below considered only gravity loads with a dead load and reduced live load of 50 psf. A uniform distributed load of 260 pounds per foot per floor was assumed for the curtain wall loading. Mathematical models were analyzed for the undamaged state, denoted ND, and three damage states, one of which corresponds to the existing damage shown in

Figure 16. Three-dimensional mathematical model of framing on lines 6, 7, and 8 for DS1.

Figure 4a. Each damage state involved the removal of columns on line 8 from tenant level 7 to tenant level 25. The three damage states involved the removal of (1) the column on line D (the observed damage per Figure 15b); (2) the columns on lines D and E; and (3) the columns in lines C, D, and E, denoted DS1, DS2, and DS3, respectively. Maximum member actions under gravity loads were calculated for the undamaged state and the three damage states.

Figures 17 and 18 present some of the results of the two- and three-dimensional analyses, respectively. Shown in these figures are moments normalized by the yield moment for the assumed beam section sizes at tenant level 25—the floor level immediately above the observed damage. The spandrel beam designation (e.g., DE) refers to the grid lines between which the beam spans (e.g., lines D and E). The girder designation (e.g., E87) refers to the grid line along which the girder is aligned (e.g., line E) and the grid lines between which the girder spans (e.g., lines 8 and 7). Such normalized moments represent demand-to-capacity (D/C) ratios for these elements, albeit not exactly, because M_y is used in lieu of ϕM_{nx} and each beam is assumed to be fully braced.

First consider damage state DS1 (the observed damage) and two-dimensional analysis. All D/C ratios are substantially less than 1. The three-dimensional analysis shows similar results. These results provide an explanation for the observed behavior of the framing along line 8 after the impact of debris from tower 2 and the loss of a column on line D, namely, that the moment-resisting framing above tenant level 25 provided an alternate (redundant) path for gravity loads around line D and to the foundation without distress of the structural framing. As observed from DS1, models with increasing levels of damage (i.e., DS2 and DS3) showed that the moment-resisting framing above the damage provided an alternate path for gravity loads.

The mathematical models for damage states DS2 and DS3 were prepared to evaluate the robustness of a building frame with characteristics similar to those of 130 Liberty Plaza, where robustness herein is judged by the ability of the framing system to support gravity loads after the loss of multiple perimeter columns. The results of the two-dimensional analysis of the DS2 model show that the frame on line 8 would have been compromised by the loss of columns on lines D and E unless the moment-resisting connections were ductile (i.e., possessed some degree of inelastic rotation capacity).

Review of the three-dimensional analysis results of Figure 18, however, shows that use of the results of the two-dimensional analysis leads to conservative conclusions and that moment-resisting framing perpendicular to

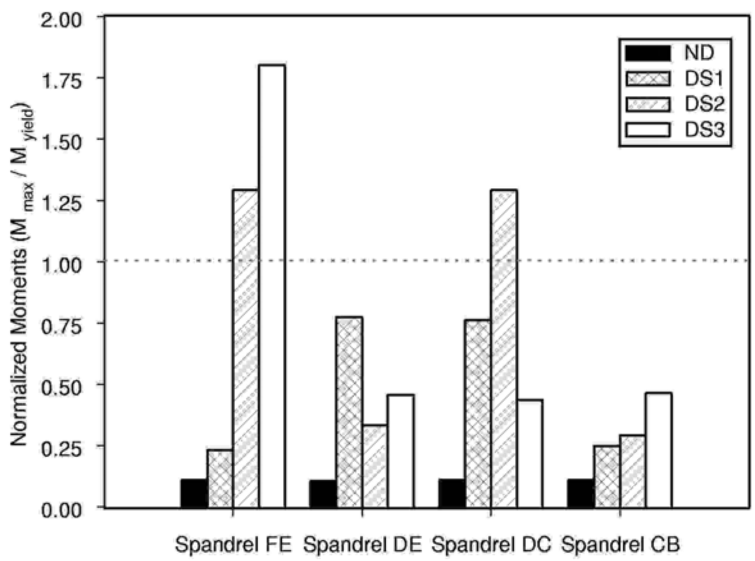

Figure 17. Demand-to-capacity ratios for two-dimensional linear elastic analysis.

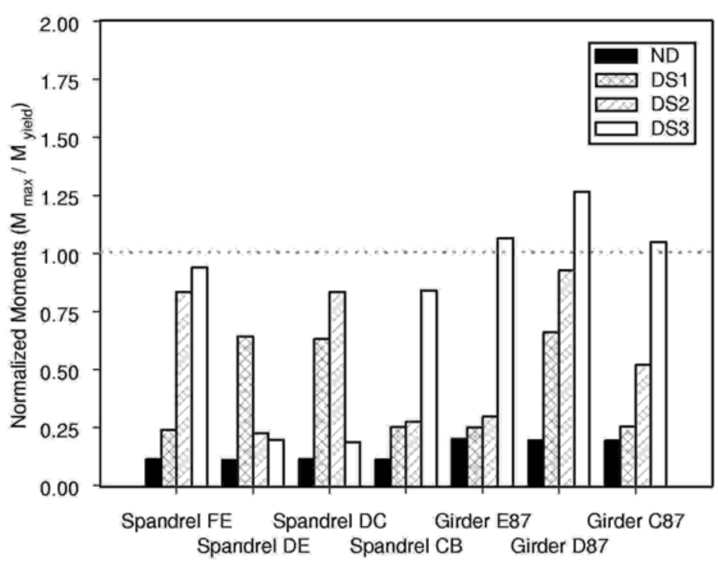

Figure 18. Demand-to-capacity ratios for three-dimensional linear elastic analysis.

line 8 also participated in the redistribution of load around the lost columns on lines D and E. Analyses for both the two- and three-dimensional models of DS3 (the loss of columns on lines C, D, and E) show modest overloads in both cases. For the three-dimensional analysis, the D/C ratios are greatest in the framing perpendicular to line 8, namely, girders C87, D87, and E87.

Demand-to-capacity ratios were calculated for columns on line 8 between tenant levels 24 and 25 (see Figure 15) for both two- and three-dimensional analyses. The column designation (e.g. F8) in Figures 19 and 20 refers to the column between tenant levels 24 and 25 at the intersection of lines F and 8. Shown in Figures 19 and 20 are column D/C ratios. These ratios were calculated using the 1998 edition of the *Manual of Steel Construction—Load and Resistance Factor Design* (American Institute of Steel Construction, 1998) nominal strength equation for members under combined forces (LRFD Eqn. H1-1a), namely,

$$\frac{P_u}{\phi P_n} + \frac{8}{9}\left(\frac{M_{ux}}{\phi M_{nx}} + \frac{M_{uy}}{\phi M_{ny}}\right) \leq 1.0 \tag{1}$$

To facilitate calculation of the D/C ratios and comparison of analysis results, the value of the effective length factor was assumed to be 1.0 for all columns. This value is the largest assuming that side-sway is prevented, which is a reasonable assumption for the moment frame considering the high lateral stiffness of the braced core (significantly greater than that of the moment frame) and the presence of rigid floor diaphragms.

The results of the two-dimensional analyses shown in Figure 19 indicate D/C ratios less than unity for the undamaged state ND and the damage states DS1 and DS2. For damage state DS3, the D/C ratios for columns F8 and B8 exceed unity. Ratios greater than unity can be attributed to an increase in both axial forces and moments due to the removal of columns C8, D8, and E8. This observed increase in bending moment for the two-dimensional analyses ranged from essentially zero for ND to approximately $0.25M_p$ for DS3, where M_p is the plastic moment. Noting that the span between adjacent columns for DS3 is four times the span in the undamaged state ND, an increase in moment demand is expected. The D/C ratios for the three-dimensional model (Figure 20) are less than unity for ND and DS1, DS2, and DS3. Again, the results of the three-dimensional analyses indicate that the use of two-dimensional analysis leads to conservative conclusions and that the presence of perpendicular framing provides additional redundancy and capability for gravity loads to be redistributed to adjacent framing.

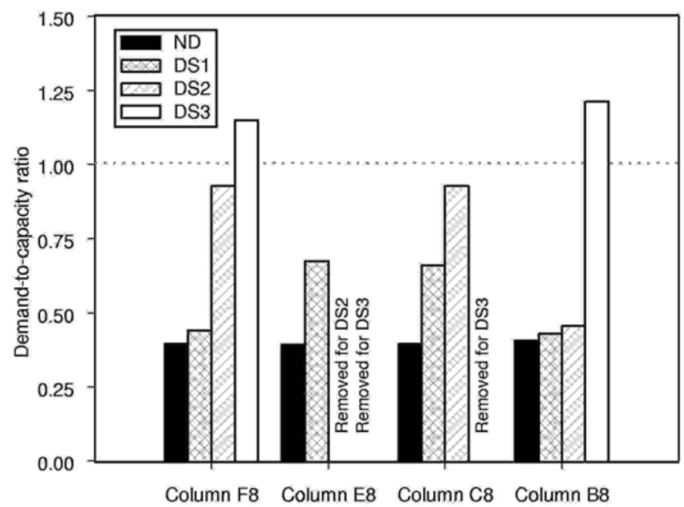

Figure 19. Demand-to-capacity ratios for two-dimensional linear elastic analysis.

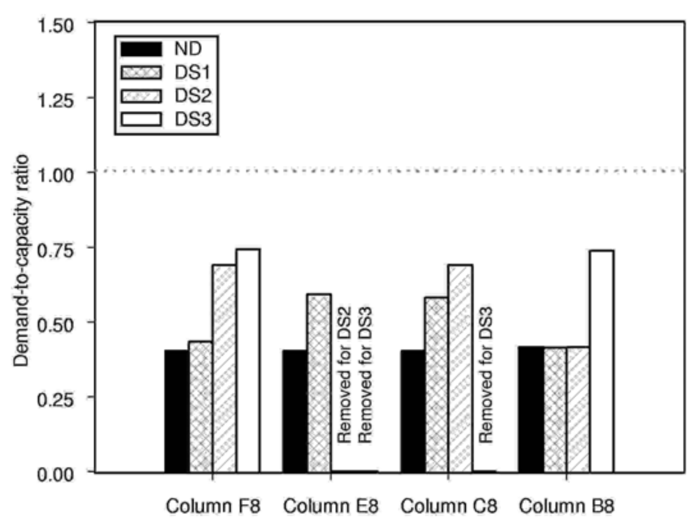

Figure 20. Demand-to-capacity ratios for three-dimensional linear elastic analysis.

Simple Plastic Analysis

Simple two- and three-dimensional plastic analyses were performed to determine an upper bound on the load-carrying capacity of the framing system for each of the three damage states identified previously. In both the two- and three-dimensional analyses, beam plastic moments were calculated assuming a yield stress of 36 ksi (kips per square inch) and the section sizes determined in the preliminary design (see Figure 2). All sections were assumed to be compact. Further, all beam-to-column connections were assumed to have unlimited rotation capacity. For the two-dimensional analyses, vertical panel mechanisms were assumed to form for each damage state. Figure 21 shows the assumed mechanism for DS1. The assumed mechanisms for the three-dimensional analyses were similar, with the addition of hinges forming in the girders of the perpendicular framing where appropriate. Curtain wall loads and beam plastic moments were taken as known quantities, and the maximum corresponding floor load that could be sustained by the framing was determined for each case. Joint mechanisms involving plastic hinges in the column above and below the beams of tenant level 25 and in the beams of adjacent bays were also considered, however, the gravity loads necessary to cause those mechanisms were found to be larger than those required to form the mechanism of Figure 21.

The results of these analyses are presented in Table 1 in terms of both the maximum floor loading (measured in psf) and the maximum floor loading normalized by the likely *maximum* loading at the time of the September 11th attacks, judged by the reconnaissance team to be approximately 100 psf.

These analyses support the results of the elastic analysis described above, namely, that the framing system could have tolerated the loss of two columns without collapse. Note the additional load-carrying capacity that results from consideration of the framing perpendicular to line 8.

However, it must be noted that the cover-plated moment-resisting connections employed in the construction of the building likely have limited plastic rotation capacity as demonstrated by a series of tests conducted after the 1994 Northridge earthquake (Kim et al., 2000). Therefore, the results of the simple plastic analyses must be interpreted with care.

Vertical Nonlinear Static Analysis

Two-dimensional nonlinear static analysis of the framing along line 8 was performed for the three damage states to obtain insight as to the displacements that could be expected at the maximum floor loads predicted by simple plastic analysis. Elastic perfectly plastic moment-rotation relationships were assumed for all beams. Connections were assumed to have infinite rotation capacity. The analyses were run using SAP2000 under displacement control and used the node at frame line D and tenant level 25 as the control node. The loading pattern was a series of equal valued point loads at the locations where the floor beams and perpendicular girders framed into the spandrel elements on line 8.

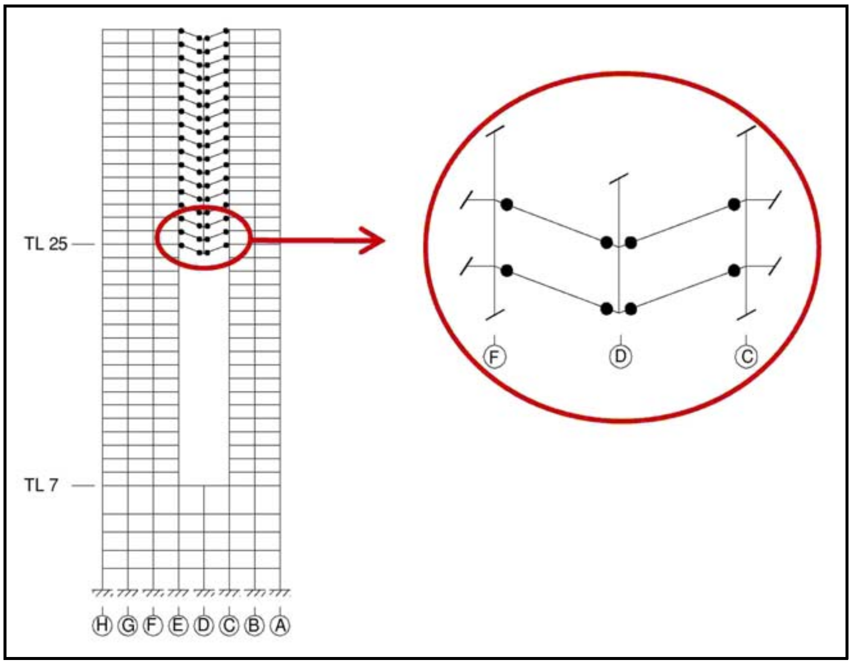

Figure 21. Two-dimensional collapse mechanism for DS1.

Table 1. Plastic analysis results.

	Two-dimensional Analysis		**Three-dimensional Analysis**	
Damage State	Floor Load (psf)	Normalized Load	Floor Load (psf)	Normalized Load
1	293	2.9	308	3.1
2	136	1.4	218	2.2
3	84	0.8	182	1.8

Before running the displacement controlled nonlinear static analysis, the curtain wall load was applied as a single force controlled step to be consistent with simple plastic analysis calculations. Figure 22 shows the observed progression of plastic hinging for DS1. The hinging patterns for DS2 and DS3 were similar to DS1. Hinging started at the beam-to-column connections on lines E and C near tenant level 25, progressed to the connections on frame line D, and then vertically up through the framing on line 8.

Figure 23 shows the resulting relationships between floor load (psf) and the deflection of line D at tenant level 25 for the three damage states, where the floor load is assumed to be present over the entire width of the damaged zone (i.e., between lines C and E for DS1, lines C and F for DS2, and lines B and F for DS3). The initial displacements seen in the figure correspond to the deflection due to the prior application of the curtain wall load. Also shown in this figure is the research team's estimate of the likely maximum floor loading at the time of the September 11th attacks, of 100 psf. As expected, an increase in damage led to increased structural flexibility and reduced the maximum permissible floor load. The results of the nonlinear static analysis and those of the simple plastic analysis are in good agreement for all damage states.

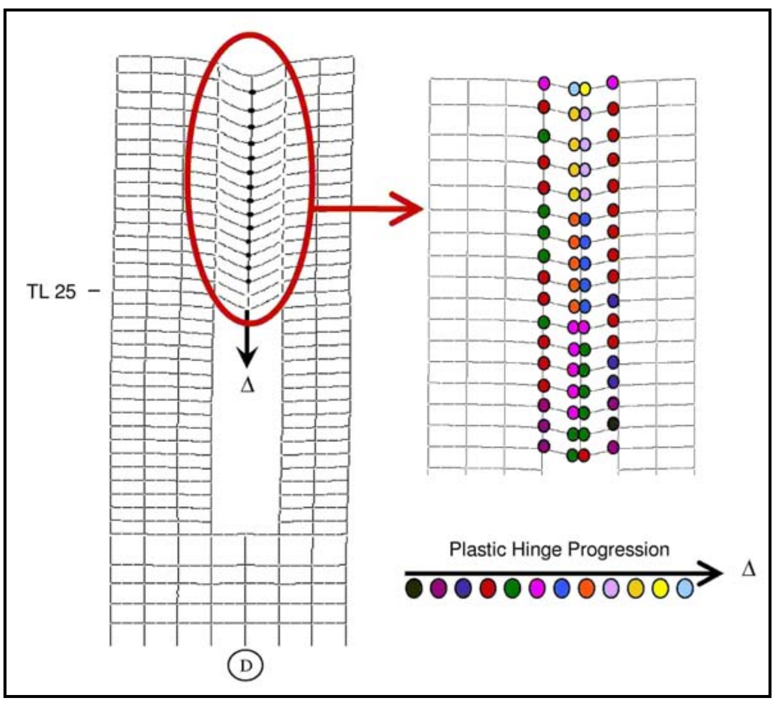

Figure 22. Progression of plastic hinge formation in DS1.

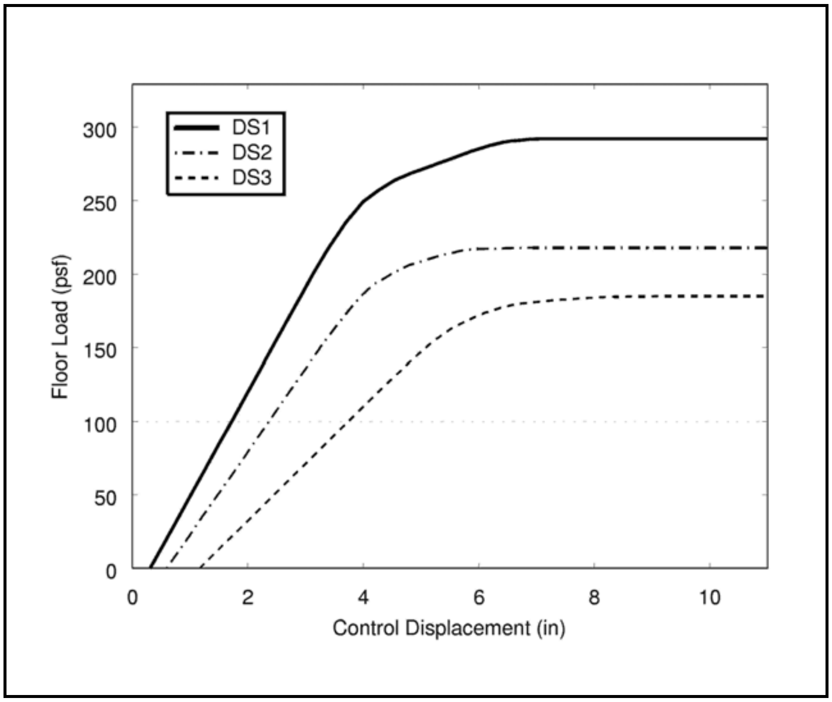

Figure 23. Two-dimensional vertical nonlinear static analysis for DS1, DS2, and DS3.

Summary and Conclusions

The 130 Liberty Street building sustained severe damage from falling debris during the collapse of the World Trade Center tower 2. Reconnaissance efforts on September 21 and 23, 2001, documented the exterior and interior damage to the building. Despite the loss of a perimeter column over a 17-story height, the building did not collapse because the lateral and gravity load resisting systems were highly redundant. The redundant structural systems permitted gravity loads to be redistributed around the badly damaged region, an observation supported by preliminary elastic and plastic analyses of a building frame with characteristics similar to those of the damaged building. Key observations from the work to date are

- Highly redundant gravity and lateral-force-resisting systems are key to the construction of damage-tolerant buildings.

- The use of ductile details (ability to deform well into the inelastic range) will improve the damage tolerance of buildings.

- Simple framing systems such as unreinforced slabs on metal decking can span substantially farther than assumed in design, and such capabilities should be included in the evaluation of buildings for damage tolerance. The addition of inexpensive details (such as continuous slab reinforcement and continuity in the metal decking) could further enhance building performance and prevent partial collapses.

- Simple two- and three-dimensional analysis tools such as those adopted for the work presented in this summary report can be used to judge, in a preliminary sense, the damage tolerance of buildings.

- Two- and three-dimensional analysis tools that are commonly used for the earthquake engineering of buildings showed that the 130 Liberty Street building could sustain the loss of an exterior column over a 17-story height as observed during the post-September 11th reconnaissance work.

References

American Institute of Steel Construction. 1989. *Manual of Steel Construction—Allowable Stress Design*. Chicago, IL: AISC.

American Institute of Steel Construction. 1998. *Manual of Steel Construction —Load and Resistance Factor Design*. Chicago, IL: AISC.

Berman, J., G. Warn, A.S. Whittaker, and M. Bruneau. 2002. *Reconnaissance and Preliminary Assessment of a Damaged Building Near Ground Zero*: *Engineering and Organizational Issues Related to the World Trade Center Terrorist Attacks*. MCEER-02-SP03. Buffalo, NY: Multidisciplinary Center for Earthquake Engineering Research, State University at New York.

Bruneau, M., A.S. Whittaker, and A.M. Reinhorn. 2002. *Overview of Damage to Buildings Near Ground Zero: Engineering and Organizational Issues Related to the World Trade Center Terrorist Attacks.* MCEER-02-SP02. Buffalo, NY: Multidisciplinary Center for Earthquake Engineering Research, State University at New York.

City of New York. 1970. *Building Code of the City of New York*. New York, NY: Van Nostrand Reinhold Company.

Computers and Structures, Inc. 2000. "SAP2000-Integrated Finite Element Analysis and Design of Structures," Version 7.4. Berkeley, CA: CSI.

Hart, F., W. Henn, and H. Sontag. 1978. *Multistory Buildings in Steel*. English translation, ISBN 0-258-969761. London: Granada Publishing Limited.

Kim, T., A.S. Whittaker, A.S.J. Gilani, V.V. Bertero, and S.M. Takhirov. 2000. "Cover-Plate and Flange-Plate Reinforced Steel Moment Connections." Report No. PEER 2000/07. Berkeley, CA: Pacific Earthquake Engineering Research Center, University of California–Berkeley.

Warn G., J. Berman, A.S. Whittaker, and M. Bruneau. Forthcoming. "Reconnaissance and Preliminary Assessment of a Damaged High-Rise Building Near Ground Zero." *The Structural Design of Tall Buildings.*

Acknowledgments

The authors wish to acknowledge the substantial technical contributions of the expert structural engineering staff at LZA Technology of New York, a division of the Thornton/Tomasetti Group. Special thanks are due to Mr. Edward Sweirtz (Associate Partner, Chicago), Mr. Daniel Cuoco (Managing Principal, New York), and Mr. Emmanuel Velivasakis (Managing Principal, New York).

This work was supported in whole by the Earthquake Engineering Research Centers Program of the National Science Foundation under a supplement to Award Number ECC-9701471 to the Multidisciplinary Center for Earthquake Engineering Research. However, any opinions, conclusions, and recommendations presented in this paper are those of the authors and do not necessarily reflect the views of the sponsors.

Correspondence should be directed to Andrew Whittaker, Associate Professor, Department of Civil, Structural, and Environmental Engineering, University at Buffalo, Amherst, NY 14260, e-mail: awhittak@acsu.buffalo.edu.